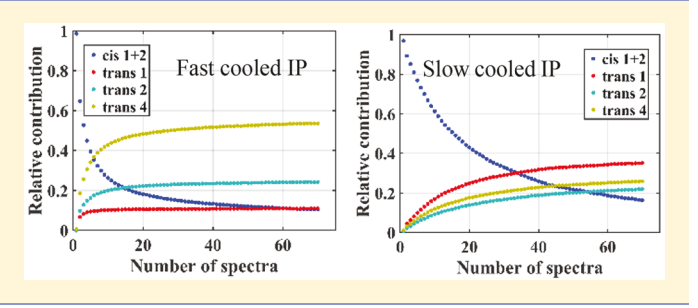
Translational Diffusion and Unstable Conformer Trapping in Glassy Isopentane at 77 K

László Zimányi,**,†© Sumesh B. Krishnan,‡ Emily Williford,‡ Shipra Gupta,‡ Jonathan Sepulveda,‡ Hadleigh Schwartz,‡ Frank B. Mallory,§ Clelia W. Mallory,§, Olga Dmitrenko, and Jack Saltiel*,‡©

Supporting Information

ABSTRACT: Diffusional quenching in isopentane (IP) glass at 77 K is demonstrated by the reduction of triphenylene phosphorescence lifetimes in the presence of 1,3-pentadiene and/or molecular oxygen. Fluorescence spectra and lifetimes of cis- and trans-1,2-di(1-methyl-2-naphthyl)ethene in IP glass at 77 K reveal that the $cis \rightarrow trans$ photoisomerization leads to the trapping of unstable conformers of the trans isomer. The claim that IP at 77 K is not sufficiently viscous to trap unstable photoproduct conformers is invalidated.



■ INTRODUCTION

One bond twist (OBT) cis-trans photoisomerization of olefins is inhibited in viscous media and in free volume limiting media generally. 1,2 The hula-twist (HT) mechanism, initially postulated to explain retinyl photoisomerization within the protein environment in rhodopsin and bacteriorhodopsin,^{3,4} involves simultaneous rotation about a double bond and an adjacent essential single bond (equivalent to a 180° translocation of one CH unit).^{3,4} It is assumed to reduce free volume requirements by confining motion to the vicinity of the isomerizing double bond. Following the conclusion that the cis-trans photoisomerization of previtamin D in EPA (5:5:1 diethyl ether/isopentane/ethanol v:v) at 90 K follows the HT mechanism,⁵ a conclusion that turned out to be erroneous,⁶ that mechanism was assumed to apply generally in organic glasses at low temperatures (T's). The photoisomerization of cis,trans-1,4-di-o-tolyl-1,3-butadiene (ct-1) in EPA at 77 K is a relevant example.¹¹ Starting as a mixture of two conformers, it gave two tt-1 conformer photoproducts. The claim to the contrary notwithstanding, 11 that study failed to distinguish between OBT and HT mechanisms because both mechanisms predict formation of the same two products. In contrast, we found that only single stable conformers of cc- and ct-1 are observed in isopentane (IP) at 77 K and we showed that they photoisomerize exclusively to stable ct- and tt-1 conformers. 12 HT requires the formation of unstable conformer photoisomers; consequently we ruled out its involvement. That conclusion was disputed on the basis that IP glass at 77 K is not sufficiently viscous to trap unstable conformers of photoisomers.¹³ The observation of I₂ formation from the

irradiation of ethyl iodide in IP at 77 K provided evidence for translational diffusion of iodine atoms. 14 Formation of solvent separated radical pairs in even more viscous glasses such as EPA was attributed to temporary local melting of the glass cage due to deposition of excess vibrational energy during the photolysis event.¹⁴ It was reasoned that the fluidity that allows translational diffusion should also prevent unstable conformer trapping in an IP glass. 13 We address here Liu's criticism of the work in ref 12. We confirm previous observations demonstrating diffusional phosphorescence quenching in IP at 77 K, 15 and we show that when cis-1,2-di(1-methyl-2-naphthyl)ethene (c-2) is irradiated in IP at 77 K, unstable conformer distributions of the photoisomer, t-2, are trapped as in methylcyclohexane (MCH) glass¹⁶ (Scheme 1).

EXPERIMENTAL SECTION

Materials. Isopentane (Sigma-Aldrich, spectrometric grade) was passed through a AgNO3 impregnated alumina column and distilled. Methylcyclohexane, diethyl ether, ethyl alcohol, t-2, and c-2 used in this work were previously described. The triphenylene (TPE) used was the same as in ref 19. trans-Piperylene (t-P, Sigma-Aldrich, reagent) was used as received.

Measurements. UV absorption spectra were recorded with a Varian Cary 300B UV-vis spectrophotometer. Fluorescence spectra and phosphorescence lifetimes were determined using

Received: August 20, 2019 Revised: September 17, 2019 Published: September 26, 2019



[†]Institute of Biophysics, Biological Research Centre, Hungarian Academy of Sciences, P.O. Box 521, Szeged, Hungary, H-6701

^{*}Department of Chemistry and Biochemistry, Florida State University, Tallahassee, Florida 32306-4390, United States,

[§]Department of Chemistry, Bryn Mawr College, Bryn Mawr, Pennsylvania 19010, United States

Department of Chemistry, University of Pennsylvania, Philadelphia, Pennsylvania 19104, United States

 $^{^{\}perp}$ Department of Chemistry and Biochemistry, University of Delaware, Newark, Delaware 19716, United States

Scheme 1. Photoisomerization of c-2 Conformers in MCH Glass at 77 K

a Horiba Fluoromax 4 fluorometer equipped with a phosphoroscope accessory. Excitation and emission slit widths were set at 2.0 nm. Emission spectra were measured with $\lambda_{\rm exc}$ = 256 nm for the 330-510 nm range. Triphenylene phosphorescence lifetimes were measured with $\lambda_{\rm exc}$ = 256 nm and $\lambda_{\rm mon}$ = 458 nm with 0.1 s time intervals over 100 s. The shutter was opened and closed manually. Each reported lifetime is the average of three to five measurements. Fluorescence lifetimes were determined using a second Horiba Fluoromax 4 instrument equipped with a time-correlated single-photon counting accessory and an R928 PMT detector (Hamamatsu). The light sources were 295 and 370 nm nanoLEDs (Horiba) having a pulse duration of <0.75 ns and 1 MHz repetition rate. Photon count was set at 10 000 and the time-to-amplitude converter range was 50 ns. The instrument response functions were obtained by collecting Rayleigh scatter at 295 and 370 nm. The fluorescence lifetime values were determined by reconvoluting the instrument response function with exponential decay using DAS6 (Horiba) fluorescence decay analysis software. The quality of the fits was judged by χ^2 values, standard deviations of derived lifetimes, and visual inspection of the residuals. Samples, 0.5 mL, were contained in cylindrical (2 mm inside diameter) quartz NMR tubes immersed in liquid nitrogen in the Dewar of the phosphorescence accessory of a Hitachi F-4500 fluorometer. For phosphorescence measurements the quartz NMR sample tubes were equipped with standard taper joints and grease traps. After degassing with a vacuum system (at least four freeze-pump-thaw cycles) to $<10^{-4}$ Torr, the tubes were sealed at a constriction.

The effect of oxygen on TPE phosphorescence was evaluated in MCH, IP, and EPA glasses at 77 K. A stock solution of TPE, 1.0×10^{-3} M, was prepared in MCH. Aliquots, 40 μ L, of this solution were delivered to three 5 mL volumetric flasks. In one, the volume was made up with MCH, and in the other two the MCH was removed and the volumes were made up with IP and EPA, respectively, resulting in 8.0 × 10⁻⁶ M working solutions. Aliquots, 0.70 mL, were delivered into quartz NMR tubes. For each solvent, one tube was left open to air, one was outgassed with N2, and one was outgassed with O₂ before plunging into the liquid N₂ Dewar for phosphorescence and phosphorescence lifetime measurements. The same TPE solution and procedure were used for the t-P quenching experiments except that each set of the final 5 mL flasks also contained 15, 25, 35, and 45 μ L of a 0.992 × 10⁻¹ M t-P stock solution (10 µL of t-P in 1.0 mL of MCH, IP, or EPA). The procedure used for the c-2 and t-2 fluorescence measurements was as previously described. 16,17 As in MCH glasses at 77 K, t-2 conformer mixtures trapped in IP glasses are stable during the fluorescence measurements, whereas trapped c-2 conformer mixtures progressively photoisomerize

to *t*-2 due to light exposure during the acquisition of each fluorescence spectrum. Under our conditions, sequential measurement of fluorescence spectra over a period of 1 h leads to almost complete conversion to *t*-2 in the small volume of the sample that is exposed to the excitation light. During the photoreaction the content of *t*-2 increases as each fluorescence spectrum is acquired. The only departure from previous work ^{16,17} is that, before entering such spectra into a spectral matrix for singular value decomposition (SVD) analysis, they were corrected for the distortion due to the increasing contributions of the *t*-2 conformers. The procedure used in performing this correction is described in the Supporting Information.

Computational Methods. Fully optimized calculated geometries of the conformer structures of t-2 and of trans-1,2-di(2-naphthyl)ethene, t-3, the parent, were available from previous work. 16 Gas phase conformer electronic spectra based on those structures were calculated using time dependent density functional theory (TD DFT) calculations. 20,21 A total of 24 excited states and their corresponding oscillator strengths were determined. The spectra were simulated using GaussSum 2.2. The equation employed to calculate theoretical spectra is based on Gaussian convolution as reported in the open source code of the program (available at http://gausssum.sourceforge. net/GaussSum UVVis Convolution.pdf). The full-width at half-maximum value of 3000 cm⁻¹ was used to obtain simulated spectra. The excited state calculations were performed on the B3LYP/6-311+G(d,p)-optimized structures using the TD DFT method, ^{23–26} namely, TD CAM-B3LYP/6-311+G(d,p). Caricato and coauthors have reported that the CAM-B3LYP short-long-range separated functional performs on average better than the other functionals in reproducing the reference results (EOM-CCSD) for simulation of spectra.²

RESULTS

Phosphorescence Quenching. Emission spectra and phosphorescence lifetimes were measured using different samples of air saturated MCH, EPA, and IP solutions of TPE (8×10^{-6} M) cooled to 77 K. Fluorescence intensities were the same in MCH and EPA and there was a small (7%) drop in intensity in IP, but the phosphorescence intensity and lifetime were significantly diminished in IP. Emission spectra with normalized fluorescence intensity are shown in Figure 1. It is evident that the phosphorescence intensity is diminished

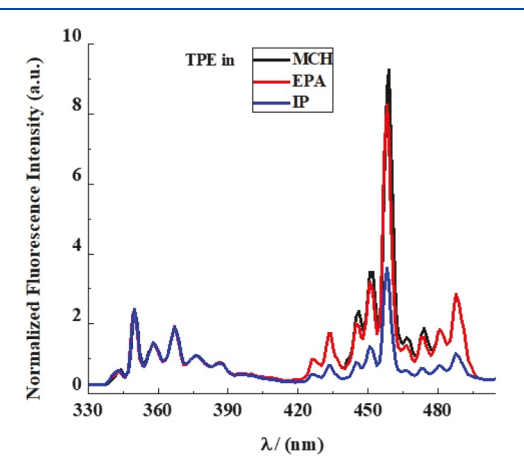


Figure 1. TPE emission in air-saturated MCH (black), EPA (red), and IP (blue) at 77 K, $\lambda_{\rm exc}$ = 256 nm.

by a factor of \sim 3 in IP relative to MCH. The effect of oxygen concentration on TPE phosphorescence intensity in IP at 77 K is shown in Figure 2. In a separate experiment, the TPE

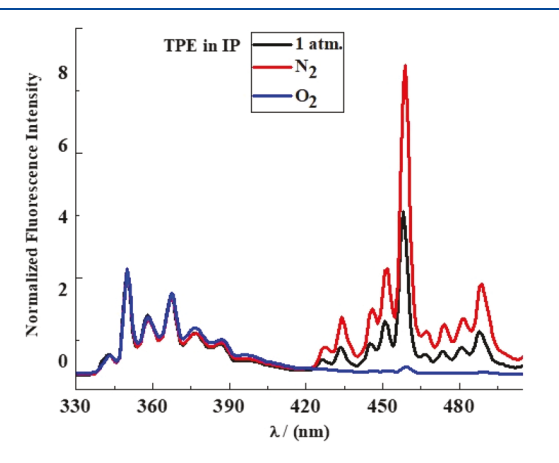


Figure 2. $[O_2]$ effect on TPE emission intensity in IP (blue) at 77 K, $\lambda_{\rm exc} = 256$ nm.

phosphorescence lifetimes measured in air saturated MCH, EPA, and IP glasses at 77 K were 14.9 ± 0.2 , 15.0 ± 0.2 and 10.3 ± 0.4 s, respectively. Outgassing the MCH solutions with N_2 and O_2 prior to immersing in liquid N_2 resulted in TPE phosphorescence lifetimes of 15.1 and 14.7 s, respectively. The outcome was very different in IP, where the same procedure yielded TPE triplet lifetimes of 12.4 and 0.46 s. The corresponding decrease in phosphorescence intensity was 38-fold. TPE phosphorescence lifetimes in degassed solutions at 77 K are shown in Table 1 as a function of [t-P].

Table 1. Effect of t-P on TPE Phosphorescence Lifetime at $77~\mathrm{K}$

		$ au_{ m p}/{ m s}$		
$10^4[t-P]/M^a$	MCH	EPA	IP	$10^4[t-P]/M^c$
0	14.8	17.2	12.4 ^b	0
0.99	14.6	17.3		
2.98	14.5	17.1	6.4	3.93
4.96	14.6	17.6	4.9	6.54
6.94	14.5	17.6	3.6	9.16
8.93	14.7		2.9	11.8

^aConcentrations at 21 °C. ^bThis value is for N₂-outgassed IP solution. ^cConcentrations corrected for IP contraction at 77 K; see text.

Fluorescence Spectra of t-2 and c-2. Fluorescence spectra of t-2 with $\lambda_{\rm exc}$ in the 300-370 nm range with 5 nm increments in IP solution at 25 °C are shown in Figure 3. Fluorescence spectra of t-2 with $\lambda_{\rm exc}$ in the 300–370 nm range (10 and 2 nm increments for 300-350 and 350-370 nm, respectively) in IP glasses obtained by fast (sample plunged into liquid nitrogen) and slower (sample slowly immersed into liquid nitrogen) cooling to 77 K are shown in Figure 4. The spectra in Figure 4 are shown normalized to unit area in Figure S3. Fluorescence spectra of c-2 with $\lambda_{\rm exc}$ in the 300–350 nm range in IP glasses obtained by fast and slower cooling (FC and SC) to 77 K are shown in Figure 5a. The slight shift in the spectra can be seen in the corresponding normalized spectra shown in Figure 5b. Spectra were recorded by scanning the emission wavelength in the 340-590 nm direction. Scanning fluorescence in the opposite direction reveals the buildup of *t*-2

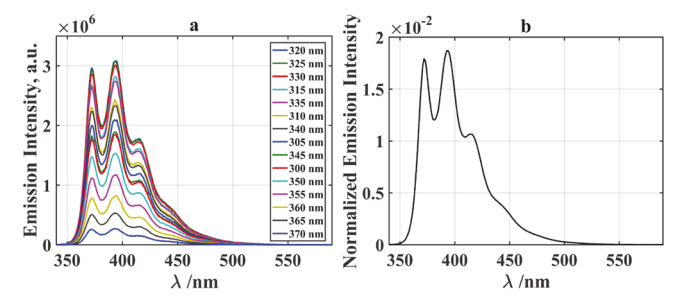


Figure 3. (a) Fluorescence spectra of t-2 in IP solution at 25 $^{\circ}$ C and (b) single component from the spectral matrix in (a).

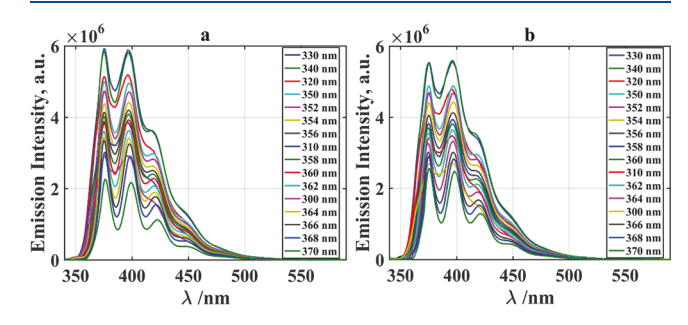


Figure 4. Fluorescence spectra of t-2 in FC (a) and SC (b) IP at 77 K for $\lambda_{\rm exc}$ in the 300–370 nm region. Vibronic structure becomes better defined as $\lambda_{\rm exc}$ is increased.

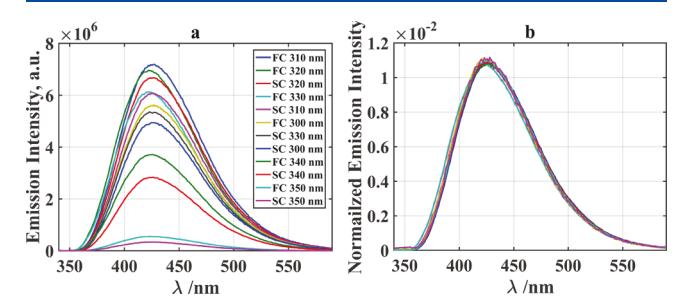


Figure 5. (a) Combined fluorescence spectra of c-2 in FC and SC IP at 77 K with $\lambda_{\rm exc}$ in the 300–350 nm range in 10 nm increments; (b) normalized spectra.

in the course of the first scan (Figure S4). Prior to SVD treatment the spectra were corrected for increasing contamination by the fluorescence of *t*-2 photoproduct (see Supporting Information). This correction is most important for the first four scans (Figure 6) and diminishes as the scans progress. Starting with pure *c*-2, uninterrupted sequential measurement of fluorescence spectra slowly converts *c*-2 to *t*-2.

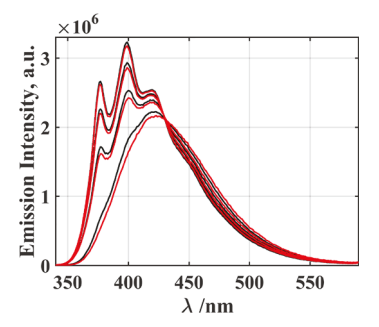


Figure 6. First four scans of c-2 in FC IP with $\lambda_{\rm exc}$ = 300 nm, experimental and corrected spectra in black and red, respectively.

Sets of corrected spectra with $\lambda_{\rm exc}$ = 300 nm in FC and SC IP at 77 K are shown in Figure 7. Sets of spectra were also

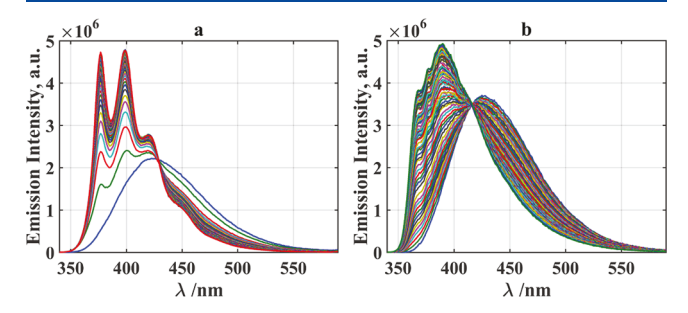


Figure 7. Corrected fluorescence spectra showing the photoisomerization of c-**2** in FC (a) and SC (b) IP at 77 K with $\lambda_{\rm exc}$ = 300 nm.

obtained monitoring the photoisomerization of c-2 with $\lambda_{\rm exc}$ = 330 nm in FC and SC IP at 77 K. The photoisomerizations were deemed complete when succeeding scans led to no apparent change in the fluorescence spectrum.

Upon completion of the c-2 \rightarrow t-2 conversions, fluorescence spectra were measured as a function of $\lambda_{\rm exc}$ as described above starting with t-2. Spectra for SC and FC IP photoproducts obtained with $\lambda_{\rm exc} = 300$ nm are shown in Figure 8. All such spectra from $\lambda_{\rm exc} = 300$ (two FC and two SC) and 330 nm (one FC and one SC) c-2 \rightarrow t-2 experiments were treated together (Figure 9).

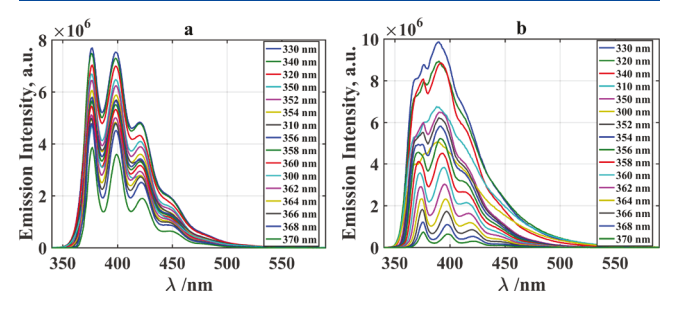


Figure 8. Fluorescence spectra of *t*-2 from *c*-2 in FC (a) and SC (b) IP at 77 K for $\lambda_{\rm exc}$ in the 300–350 nm range with 10 nm increments and in the 350–370 nm range with 2 nm increments.

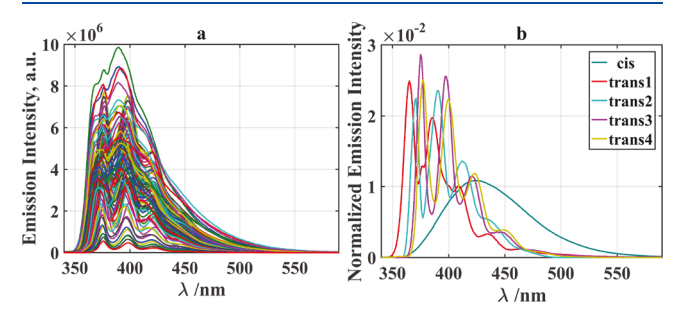


Figure 9. (a) As in Figure 8 except all spectra from all experiments are included (see text). (b) Iteratively derived pure component spectra to fit the spectra in (a) (see text).

Fluorescence Lifetimes of t-2 in IP at 77 K. Fluorescence decay from t-2 and c-2 samples was monitored at different emission wavelengths, $\lambda_{\rm em}$, in the 380–460 nm range (20 nm increments) using $\lambda_{\rm exc}$ = 295 and 370 nm. The

fluorescence decay curves are shown in Figures S5 and S6, respectively.

Calculated UV-Vis Absorption Spectra of t-2 and t-3 Conformers. Calculated coordinates and structures for the conformers of t-2 and t-3 are provided in the Supporting Information for ref 16. The structures are reproduced here for easy reference in Charts S1-S3. We retain the previously used naming scheme with subscripts A, B, and C designating strans, s-trans, s-cis, s-trans, and s-cis, s-cis conformers, respectively. The analogy with diene nomenclature holds because the C_1C_2 bonds of the naphthyl moieties are shorter than the C₂C₃ bonds. The t-2 conformers are not planar. They differ in the sense of the rotation of the ethylene plane away from the planes of the naphthyl groups, designated "+" and "-" in Charts S1-S4 per the Klyne-Prelog convention for clockwise rotation and counterclockwise rotation, respectively ("+" refers to clockwise rotation from eclipsed, taken as 0° , "–" to counterclockwise rotation). The calculated spectra of t-3 and t-2 are shown in Figure 10, parts a and b, respectively.

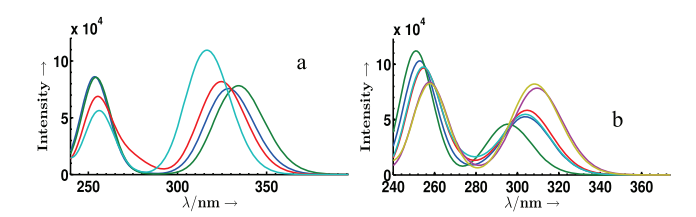


Figure 10. (a) Theoretical absorption spectra of t- $\mathbf{3}_{A}$ (cyan), t- $\mathbf{3}_{B}$ (red), helical t- $\mathbf{3}_{C}$ (blue), and planar t- $\mathbf{3}_{C}$ (green). (b) Theoretical absorption spectra of t- $\mathbf{2}_{C}$ (blue), t- $\mathbf{2}_{C'}$ (green), t- $\mathbf{2}_{B}$ (red), t- $\mathbf{2}_{B'}$ (cyan), t- $\mathbf{2}_{A}$ (purple), and t- $\mathbf{2}_{A'}$ (yellow).

DISCUSSION

Translational Diffusion. Reported TPE phosphorescence lifetime values of 15.9^{29}_{1} $16^{30,31}_{1}$ and 16.5^{32}_{2} in EPA and 14 s³² in MCH at 77 K agree well with the values in Table 1. Those lifetimes are essentially unaltered by the presence of O₂ or trans-1,3-pentadiene, and we can safely conclude that there is little, if any, intermolecular TPE triplet quenching in those relatively rigid glasses. On the other hand, in glassy IP the presence of O2 leads to pronounced decreases in TPE phosphorescence intensity, I, and lifetime, τ . The results are not strictly reproducible. Values of $I_0/I = 1.9$ and 38 were observed for air-saturated and O2-bubbled solutions. The concentration of O2 in IP is not known, but it can be estimated by using the solubility of O_2 in pentane, 1.78×10^{-2} M for 760 Torr of O₂.³³ In the presence of air, the concentration of O₂ drops to 6.97×10^{-4} M because, due to the high partial pressure of IP, 34 the partial pressure of O2 drops to 29.8 Torr at 22 °C (see the Supporting Information for the procedure used to calculate $[O_2]$). If the value in the presence of air were correct, a 25.5-fold increase in [O₂] for the O₂-bubbled glass should increase I_0/I to 25. The somewhat larger observed value of 38 may indicate that the room temperature [O₂] is augmented by partial liquefaction of the O₂ atmosphere above the solution. Lifetimes confirm the large O₂ quenching effect. Monoexponential TPE phosphorescence decay for the cooled O₂-bubbled IP glass gave a lifetime of 0.46 s. IP has been reported to form a stable glass on cooling to 77.5 K.35 However, our results reveal variability in the IP medium that is achieved on cooling to 77 K. For example, we observed biexponential TPE phosphorescence decay starting with an airsaturated solution with approximately equal contributions of 8.8 and 17.2 s lifetimes. It appears that translational O₂ diffusion in the glassy portion of IP gives the 8.8 s lifetime, whereas O2 diffusion is prevented in a more ordered, possibly crystalline, IP environment in which the 17.2 s lifetime is obtained. The observation of diffusional quenching is consistent with the Porter study¹⁴ and with a report of suspected O₂ quenching of triplet states in IP at 77 K.³⁶

The most convincing evidence of quenching by translational diffusion in the IP glass was the report of Stern-Volmer quenching of toluene phosphorescence intensity by cispentadiene. 15 Our observation of TPE phosphorescence quenching by t-P in IP at 77 K is consistent with that study and eliminates the possibility of a static component to the quenching. Decay curves of TPE phosphorescence in MCH, EPA, and IP glasses at 77 K are shown in Figure S1. The quantitative treatment of the lifetimes in Table 1 requires correction of the room temperature [t-P] values for the pronounced contraction of IP on cooling to 77 K. Although the contraction of IP is not known, contraction values have been reported for two isopentane/3-methylpentane mixtures and for 3-methylpentane (3MP).³⁷ Using those measurements, a contraction value of 0.7579 for IP was calculated by extrapolation of the plot of contraction vs 3MP mole fraction (see Figure S2). That value was used to calculate the corrected [t-P] values that are given in the last column of Table 1. The plot of the inverse of the TPE phosphorescence lifetime against

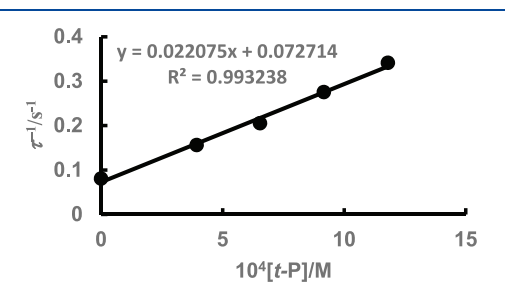


Figure 11. Effect of [t-P] on the TPE triplet lifetime in IP at 77 K.

[t-P], Figure 11, gives $\tau_p^{\circ} = 13.8 \text{ s}$ and $k_q = 2.2_1 \times 10^2 \text{ M}^{-1} \text{ s}^{-1}$,

$$(\tau_{\rm p})^{-1} = (\tau_{\rm p}^{\circ})^{-1} + k_{\rm q}[t-P]$$
 (1)

where $au_{p}^{\,\,\circ}$ is the TPE triplet lifetime in the absence of quencher and $k_{\rm q}$ is the quenching rate constant. Not surprisingly, the derived $\tau_{\rm p}^{\,\circ}$ value is larger than the 12.4 s experimental value for N2 outgassed IP, but it agrees with the observed values in MCH (Table 1). The discrepancy probably reflects imperfect O2 outgassing. Relying only on the values for degassed solutions in Figure 11 gives τ_p° = 17.5 s. Corrected for IP contraction, the quenching of toluene phosphorescence by *c*-P in the Froehlich and Morrison paper gives $k_0 = (2.0_4 \pm 0.2_3) \times$ 10² M⁻¹ s⁻¹, a value that within experimental uncertainty is identical to ours. In view of the large difference in the molecular sizes of toluene and triphenylene, the triplet energy donors used in the two studies, the near identity of the $k_{\rm q}$ values indicates that diffusion is limited to the 1,3-pentadiene quenchers. A rough estimation of the O_2 quenching rate constant gives $k_q^{\text{ox}} = 9.8 \times 10^2 \text{ M}^{-1} \text{ s}^{-1}$. In view of the fact that spin statistics limit O2 triplet quenching in solution to 1/9 of the diffusion controlled rate constant, 38 the observation of faster quenching by O_2 than by t-P is noteworthy. It probably reflects much faster diffusion by O2 in the IP glass due to its smaller size. Spin state equilibration due to the longer lifetimes of TPE/O2 encounter pairs may also contribute.

Froehlich and Morrison used the slip limit of the Debye equation³¹ and $\eta = 3 \times 10^4$ P for the viscosity of glassy IP at 77 K to calculate $k_{\text{dif}} = 569 \text{ M}^{-1} \text{ s}^{-1}$ as the rate constant for a diffusion controlled reaction. Actually, independent measurements of the viscosities of glassy IP/3MP mixtures at 77 K give an extrapolated value for pure IP of $\eta = 1.0 \times 10^6 \text{ P.}^{35-37}$ Use of that value in the slip limit of the Debye equation gives $k_{\rm dif}$ = $17~\ensuremath{\mathrm{M}^{-1}}~\ensuremath{\mathrm{s}^{-1}}$, which is more than an order of magnitude smaller than the observed values. The failure of sheer viscosity, a macroscopic property, to serve as a reliable measure of the medium's influence on molecular diffusion, even in fluid solution, has long been appreciated.³⁸ It led one of us to define microviscosity based on experimental diffusion coefficients.³⁹ In the glassy IP medium the failure of sheer viscosity is spectacular. Clearly established is that diffusional quenching does not take place in the more rigid EPA and MCH glasses. With an estimated $\eta = 10^{17}$ P value, 35 based on extrapolation of the Rosengren data, 37 glassy MCH at 77 K is enormously more viscous than IP. Again based on extrapolation of the T dependence, the viscosity of EPA at 77 K is only 2-3 orders of magnitude larger than that of IP, 40 but even that is sufficient to prevent *t*-P diffusion (Table 1).

Conformer Trapping. The well-studied behaviors of c-2 and t-2 in MCH glass at 77 K render them an ideal choice for determining whether unstable conformer distributions can also be trapped in IP glass at 77 K. The two t-2 structures in Scheme 1 are designated s-trans, s-trans and s-trans, s-cis. Steric effects due to methyl substitution lead to significant departure from planarity in both. Consequently, calculated structures [B3LYP, 6-311+G(d,p) basis set] reveal that in the ground state each exists as two enantiomeric pairs that differ in relative direction of rotation of the naphthyl groups away from the central double bond plane. 16 The calculated structures of the s*trans,s-trans* conformers (+tE+t and +tE-t) are shown in Chart 8 of ref 16. Their relative calculated gas phase free energies are 0 and 0.59 kcal/mol. 16 The corresponding structures for the s*trans,s-cis* conformers (+tE+c and +tE-c) are shown in Chart 1 with relative calculated gas phase free energies of 2.5 and 2.8 kcal/mol. 16 The great sensitivity of the fluorescence spectra of t-2 in MCH glass at 77 K to $\lambda_{\rm exc}$ was attributed to different fluorescence contributions from these four conformers. We will

Chart 1. Structures for s-trans,s-cis Conformers^a

$$t$$
-2_B 1.7 (2.5) (+ cE - t)
 $d_1 = +/-41.6^{\circ}$ $d_2 = -/+150.9^{\circ}$
 $d_1 = +/-39.7^{\circ}$ $d_2 = +/-154.2^{\circ}$

 a Numbers are ZPE $_{\rm rel}$ and (in parentheses) $G_{{\rm rel}_{4/6}^{
m p}}$ both in kcal/mol; d_1 and d_2 are the naphthyl/vinyl dihedral angles.

show below that four conformers also contribute to the fluorescence of *t*-2 in IP glass at 77 K (Figure 4).

Fluorescence Spectra of t-2 in IP Solution at 25 °C. The $\lambda_{\rm exc}$ independent fluorescence spectra of t-2 in IP solution at room temperature (RT) (Figure 3) stand in sharp contrast to the observations in the low T glasses. Seeking an explanation, we considered the possibility that the + + and + - s-trans,strans conformer pair cannot be distinguished in solution. Accordingly, the ground state structures of the +tE+t and +tE-tt conformers and the transition state (TS) for their interconversion were optimized at the RB3LYP/6-311+G(d,p) level of theory. As expected, the structure of the TS is almost planar on one side (dihedral angle = 173.6°). Those ground state geometries were taken to TD CAM-B3LYP/6-311+G-(d,p), and single-point calculations were performed to obtain vertical excitation energies without geometry optimization (details are provided in the Supporting Information). Using the vertical energies for the first bright singlet excited states leads to the conclusion that the TS for conformer equilibration that corresponds to 2.0 kcal/mol in S₀ is an energy minimum in S₁. This is consistent with the known adherence of s-trans,strans and s-trans,s-cis conformers to Havinga's nonequilibration of excited rotamers principle. 41-43 The naphthyl/vinyl bonds acquire double bond character on excitation forcing the molecules to approach planarity. It would not be surprising, therefore, if excitation of + + and + - conformers led either to their very rapid interconversion or to a common excited state in solution. However, because in the low T MCH glass distinct + + and + - conformer fluorescence spectra can be resolved, ¹⁶ we must conclude that the glassy medium traps them in excited state geometries that maintain ground state characteristics. The analysis of our results below shows that the same conclusion applies in the low T IP glass.

Fluorescence Spectra of t-2 in IP Glass at 77 K. SVD treatment of a combined matrix of the fluorescence spectra of t-2 in FC and SC IP glasses (Figure 4) revealed a robust four-component system. The evolution of eigenvector combination coefficients, as $\lambda_{\rm exc}$ is varied, is shown in Figure 12a. Circles are

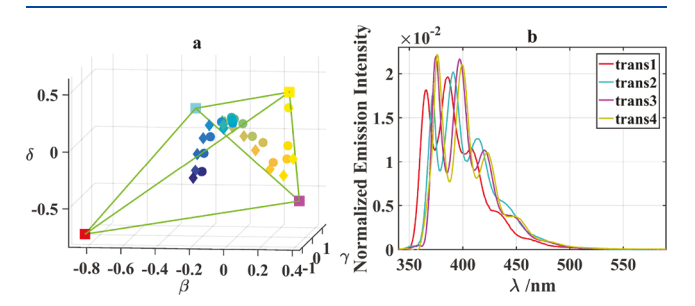


Figure 12. (a) Combination coefficients of V_{β} , V_{γ} , and V_{δ} eigenvectors for the spectra in Figure 4 and the pure component spectra in (b).

for FC and diamonds are for SC spectra. The points are color coded from blue to yellow as $\lambda_{\rm exc}$ is increased. The corners of the tetrahedron, obtained by self-modeling, are the combination coefficients of the pure component spectra shown in Figure 12b. This result is similar to that obtained in MCH glass, ¹⁶ and the derived four spectra are tentatively assigned to the two +tE+t and +tE-t and +tE+c and +tE-c conformer pairs. Although the blue shift of the red pure component spectrum is obvious in Figure 12b, the differences between the other three spectra are more subtle. We cannot rule out,

therefore, the possibility that they reflect differences in the fluorescence spectrum of one or two t-2 conformers due to different IP cage environments. The conformer distributions trapped by the IP glass are thermally and photochemically stable—the initial $\lambda_{\rm exc}=300$ nm spectrum is identical to the 300 nm spectrum measured after stepping $\lambda_{\rm exc}$ from 300 to 370 nm. The differences in spectra obtained in FC and SC IP glasses are reflected in different $\lambda_{\rm exc}$ trajectories of the combination coefficient points in Figure 12a. The conformer distribution obtained is sensitive to the manner in which the glassy medium was prepared. Furthermore, because the glass preparations were not strictly controlled, there is some irreproducibility in results from duplicate experiments. Figure 13 shows plots of the relative conformer contributions in FC

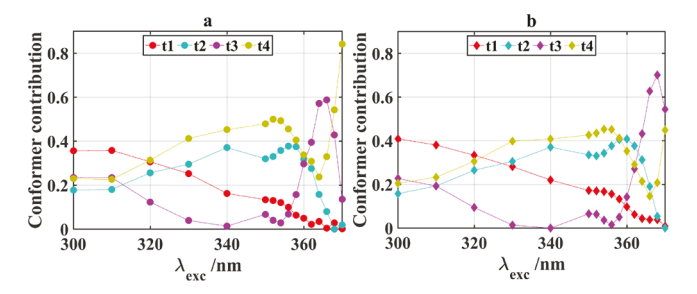


Figure 13. Percent contributions of pure t-2 conformer spectra as a function of $\lambda_{\rm exc}$ in FC (a) and SC (b) IP glasses.

and SC IP glasses, respectively. The differences are subtle except at $\lambda_{\rm exc}=370$ nm for which the yellow spectrum is dominant in FC IP, whereas the magenta and yellow spectra contribute almost equally in SC IP. Figure S7 shows the principal eigenvectors, and Figures S8–S10 show the other three combination coefficient tetrahedra.

Fluorescence Lifetimes of t-2 Conformers in IP Glass at 77 K. Excellent biexponential fits were obtained for the decay curves in Figure S5 as indicated by a 1.01–1.21 range of χ^2 values. Lifetimes and percent contributions are given in Tables S1 and S2 for $\lambda_{\rm exc}$ = 370 and 295 nm, respectively. Those excitation wavelengths coincide almost exactly with the limits of the 300–370 nm range in Figure 13. With $\lambda_{\rm exc}$ = 370 nm, the dominant lifetime (63–91%, depending on λ_{em}) in FC IP of 1.56 ± 0.12 ns can be assigned with confidence to the yellow spectrum, trans4, in Figures 9b and 12b. This conclusion is confirmed in Figure 13, where trans4 is seen to contribute more than 80% of the fluorescence area with $\lambda_{\rm exc}$ = 370 nm. As the most red-shifted spectrum, it is probably due to one of the s-trans,s-trans conformers of t-2. Analysis of the decay curves obtained in SC IP with $\lambda_{\rm exc}$ = 370 nm gives similar contributions of two lifetimes, 1.56 \pm 0.09 and 1.97 \pm 0.11 ns (Table S1). Based on Figure 13, the magenta spectrum can be assigned the 1.97 ns lifetime. As the two most red-shifted spectra, we tentatively assign the yellow and magenta spectra to the two *s-trans,s-trans* conformers of *t-***2**. According to Figure 13, all four conformers contribute with $\lambda_{\rm exc}$ = 300 nm and are likely to contribute in the decays with λ_{exc} = 295 nm. Table S2 shows that we observe three lifetimes: 1.13 ± 0.10 , 1.54 ± 0 . 05, and 2.20 \pm 0.18 ns. Assuming that the latter two can be assigned to the yellow and magenta spectra, respectively, the 1.13 ± 0.05 ns lifetime must be due to one or both of the scis,s-trans conformers of t-2.

"Pure" c-2 Fluorescence Spectra in IP at 77 K. Fluorescence spectra obtained from the first scan by exciting

c-2 in FC and SC IP glass are structureless (Figure 5) provided that in each case emission wavelengths, λ_{em} , are scanned in the low to high λ_{em} direction. Buildup of t-2 is readily observed in the second scan (Figure 6) or even in the first scan when the direction of the scan is reversed (Figure S4). This apparent anomaly is resolved when one considers that t-2 fluorescence contributes more at the shorter λ_{em} 's. When scanning from 340 to 590 nm, t-2 buildup is too low to discern at short $\lambda_{\rm em}$ and t-2 does not fluoresce at long λ_{em} . Combined, these two factors minimize contamination of the c-2 fluorescence spectrum by the fluorescence of the *t*-2 photoproduct. The same two factors maximize the photoproduct contribution when the fluorescence spectrum is recorded by scanning in the 590-340 nm direction. In previous publications the distortion of fluorescence spectra due to slow continuous buildup of photoproduct in the course of each scan was ignored without seriously affecting the results of the SVD analysis. In the present work, the spectra were corrected by removing the monotonically increasing fluorescence contribution of freshly produced t-2 photoproduct (see the Supporting Information). As observed in MCH glass at 77 K, 17 the c-2 fluorescence spectra vary slightly with λ_{exc} and are a two-component system. The normalization line and derived pure component spectra based on the Lawton-Sylvestre (LS) nonnegativity selfmodeling criterion are shown in Figure 14.44,45 In view of

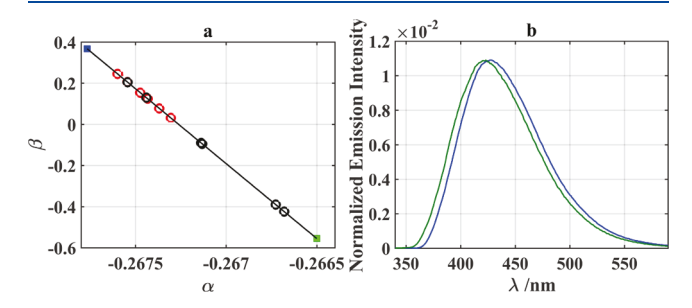


Figure 14. (a) Combination coefficients on the normalization line for pure c-2 spectra in FC (black) and SC (red) IP glasses. (b) Pure component spectra corresponding to the squares at the ends of the normalization line.

the much smaller observed shift than was expected based on the theoretical absorption spectra of the *s-trans,s-trans* and *scis,s-trans* conformers of *c-***2** in the gas phase, ¹⁷ we refrain from assigning structures to the two spectra.

Photoisomerization of c-2 to t-2 in IP at 77 K. Fast Cooled IP Experiments. In addition to the corrected spectral set in Figure 7a, we obtained an additional set for $\lambda_{\rm exc}=300$ nm and an analogous spectral set for $\lambda_{\rm exc}=330$ nm in FC IP. SVD analysis of the spectra in Figure 7a revealed a very clear rank 4 spectral matrix, whose spectra could be represented, to a good approximation, as combinations of the first two eigenvectors, consistent with an average c-2 spectrum giving an average t-2 spectrum. There are, however, small systematic deviations of the (α,β) combination coefficients from the normalization line (Figure 15a), and the true combination coefficient evolution with increasing scan number (i.e., irradiation time) is shown in Figure 15b using the three largest values of the $(\alpha,\beta,\gamma,\delta)$ sets, indicating that a spectrum corresponding to the weighted average of the c-2 conformers gives way to a mixture of three t-2 conformer spectra.

Kinetic Vector Analysis. Multiexponential fit to the kinetic vectors (V) reveals four kinetic components (Figure S11). The

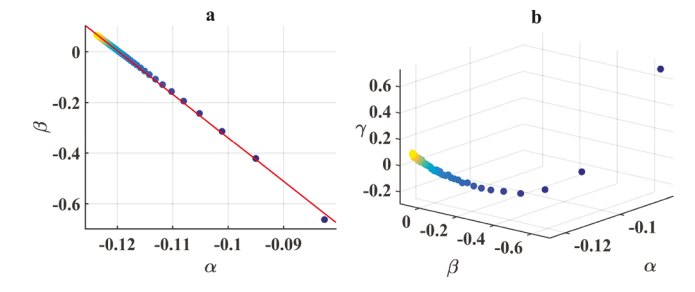


Figure 15. (a) Combination coefficients on the (α,β) normalization line for the c-2 \rightarrow t-2 spectra in Figure 7a. (b) Combination coefficients for the spectra in Figure 7a in (α,β,γ) space. The points are color coded from blue to yellow with increasing spectrum number (photoconversion time).

time base of the fit is the ordinal number of the spectra. Amplitude spectra obtained from the kinetic components (Figure 16a) allow calculation of the spectrum at the origin of

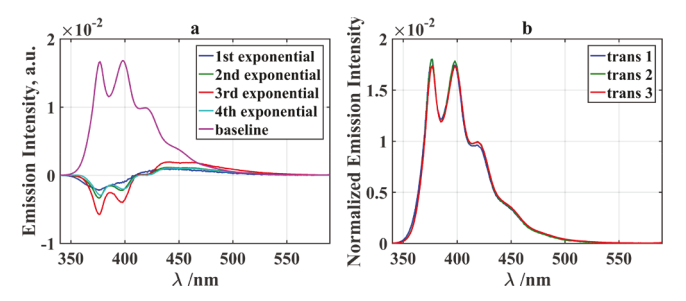


Figure 16. (a) Exponential amplitude spectra. (b) Spectra of t-2 forms produced by exponential phases 2, 3, and 4.

the consecutive exponential processes and of the t-2 products emerging from the different kinetic processes (Figure 16b). The latter are almost indistinguishable indicating no c-2 conformer discrimination as the c-2 \rightarrow t-2 reaction proceeds in four kinetic phases. To summarize, photoconversion starts from a mixture of two c-2 conformers and proceeds via four separate kinetic phases—reflecting different IP glass environments. The kinetic phases produce the same composition of t-2 conformers. Furthermore, we show below that analysis of the spectra of the photoproduct as a function of $\lambda_{\rm exc}$ reveals unreacted c-2 that must occupy IP cages that prevent c-2 \rightarrow t-2 conversion, in addition to four t-2 conformers.

Analogous analysis of the other two $c-2 \rightarrow t-2$ spectral sets gave similar results with two exceptions: (1) In the other FC 300 nm experiment the transition from the first to the second spectrum was too fast to be treated as an independent exponential process. The analysis was started with the second spectrum and a three exponential fit was performed leading to the same general conclusions as for the previous data set. (2) In the FC 330 nm experiment the first two spectra appeared contaminated with t-2 and were omitted from the analysis. Again, a rank 4 spectral matrix was obtained and up to four exponential processes produce nearly identical t-2 conformer mixture spectra and some unreacted c-2 remains.

Slow Cooled IP Experiments. As for the FC experiments, an additional SC spectral set with $\lambda_{\rm exc}$ = 300 nm and one with $\lambda_{\rm exc}$ = 330 nm were recorded. The spectra were corrected for continuous buildup of t-2, as above, but corrections were much smaller, or even negligible, compared to those observed for FC in Figure 6. This is due to a slower photoisomerization rate in

the SC samples. Apart from the spectral change from spectrum 1 to spectrum 2, the spectral sets (e.g., Figure 7b) are robust two-component systems with two kinetic phases. One 300 nm photoconversion can be fitted by two exponentials. Adherence of the (α,β) combination coefficients to the normalization line (not shown) is better than in Figure 15a. However, the other 300 nm spectral set and the 330 nm set display nonexponential, linear-looking phases.

 $\lambda_{\rm exc}$ Dependence of the Fluorescence of Photoproduct t-2 Mixtures in FC and SC IP. All 80 spectra from the six c-2 \rightarrow t-2 experiments are combined in Figure 9. Ideally, those spectra should be combinations of the pure component spectra in Figures 12b and 14b. However, the experimental spectra vary somewhat with the IP environment which is not strictly reproducible from experiment to experiment. The spectral matrix in Figure 9 behaves as a rank 6–7 system, but the small systematic spectral variations thwart traditional SVD with self-modeling (SVD-SM) treatment. Rank 6 was chosen assuming that there are two cis and four trans conformers as in the pure c-2 and t-2 samples. For comparison purposes, an approximate global solution was pursued as described below.

The normalized rank 6 reconstructed matrix was iteratively fitted in a number of cycles by the pure spectra in Figures 12b and 14b. The iterations with some manual intervention (correcting negative spectral points, for instance) gradually reshaped the pure t-2 spectra. In each iteration step the new spectra were used to fit the spectral matrix to obtain a new relative contribution of the "pure" forms to the emission spectra. Iteration was terminated when no more improvement in the revised [pure spectra] × [relative contributions] vs the experimental spectra was seen (least-squares deviation of the two matrices). The resulting effective average t-2 conformer spectra are shown in Figure 9b. Although they retain the major features of the input spectra in Figure 12b, there are noticeable deviations. For example, the shoulder at about 440 nm in the most blue-shifted trans1 spectrum in Figure 12b appears as a resolved maximum in Figure 9b. The average of the very similar pure c-2 conformer spectra (Figure 14b) was employed in the fit. Relative contributions of the spectra in Figure 9b to the products of the 300 and 330 nm photoisomerizations in FC and SC IP are shown as a function of λ_{exc} in Figure 17. The fact that compositions obtained in FC and SC IP at 77 K are strikingly different proves that the IP glass traps nonequilibrium conformer distributions. Keeping in mind that we are dealing with conformer fluorescence spectra whose relative contributions depend on two unknown properties, (1) their relative absorbance at each λ_{exc} and (2) their relative fluorescence quantum yields, some interesting conclusions are in order. Based on the calculated t-2 conformer spectra in Figure 10, it seems reasonable to conclude that the most redshifted spectrum, trans4 in Figures 9b and 12b, can be assigned to the s-trans, s-trans conformer, t-2A, and the most blue-shifted spectrum can be assigned to the s-cis,s-trans conformer, t-2_B. Switching from FC to SC IP glass reverses the relative contribution of these two conformers. FC glass strongly favors the red-shifted t-2A fluorescence, whereas the SC glass favors the blue-shifted t- $\mathbf{2}_{\mathrm{B}}$ fluorescence. If the red- and blue-shifted pure fluorescence spectra of c-2 (Figure 14b) could be similarly assigned to the s-trans, s-trans-conformer, c-2_A, and the s-cis, strans-conformer, c-2B, respectively, then the presence of as much as 78% blue-shifted spectrum in the initial FC c-2 sample and as little as 10% in the initial SC sample would lead to the conclusion that the photoisomerizations give HT photo-

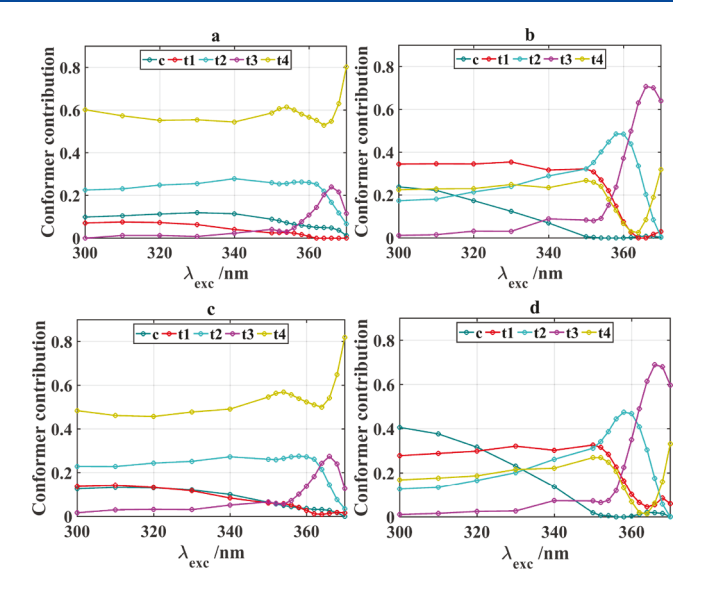


Figure 17. Fractional contributions of spectra included in Figure 9b to the product spectra of c-2 \rightarrow t-2 for 300 (a, b) and 330 (c, d) nm excitation in FC (a, c) and SC (b, d) IP at 77 K.

products. However, as pointed out above, the very small shift in the *c*-**2** fluorescence spectra precludes definitive conformer assignment and does not allow distinction between OBT and HT photoisomerization mechanisms.

Examination of Figure 17 reveals that, at 300 and 330 nm, the relatively red-shifted trans3 fluorescence spectrum makes the least contribution to the photoproduct spectra. This explains why SVD analysis of a combined matrix of fluorescence spectra measured in FC and SC IP in the course of the $c-2 \rightarrow t-2$ photoreactions reveals a four-component system. The analysis does not distinguish between the spectra of the two c-2 conformers as they proceed to the other three t-2 conformers (trans1, trans2, and trans4 in Figure 9b). The resulting reactant and product evolutions with successive spectral scan (i.e., irradiation time) are compared in Figure 18. Here also, it can be seen that at both $\lambda_{\rm exc}$'s FC favors formation of t-2_A, whereas SC favors formation of t-2_B. Figure 19a compares reaction trajectories followed by the combination coefficients of two independent 300 nm experiments and one 330 nm experiment all in FC IP. These three reactions give very similar product mixtures. Differences in the absorption spectra of the four components lead to different $\lambda_{\rm exc}$ selectivity accounting for the deviation of the 300 and 330 nm trajectories. Inclusion of the c-2 conformer spectra in the matrix is instructive. Their combination coefficients (blue and green squares in Figure 19b) cluster together with the initial spectra of the photoreaction at the lower right corner of the tetrahedron, which is arbitrarily drawn using the blue-shifted c-2 conformer spectrum as the apex. The differences in the combination coefficients of the c-2 spectra and in the 300 and 330 nm trajectories can be better appreciated in Figure 19b, a zoomed version of Figure 19a. Here, the combination coefficients of the two 300 nm experiments can be seen to cluster together above the combination coefficients of the 330 nm experiment. Vertically on the left side of Figure 19b are the combination coefficients of the c-2 spectra that are depicted as a corner of the tetrahedron in Figure 19a. Strictly speaking, if those spectra were not so similar, they would define a side of a pentahedron in combination coefficient space.

The Journal of Physical Chemistry A

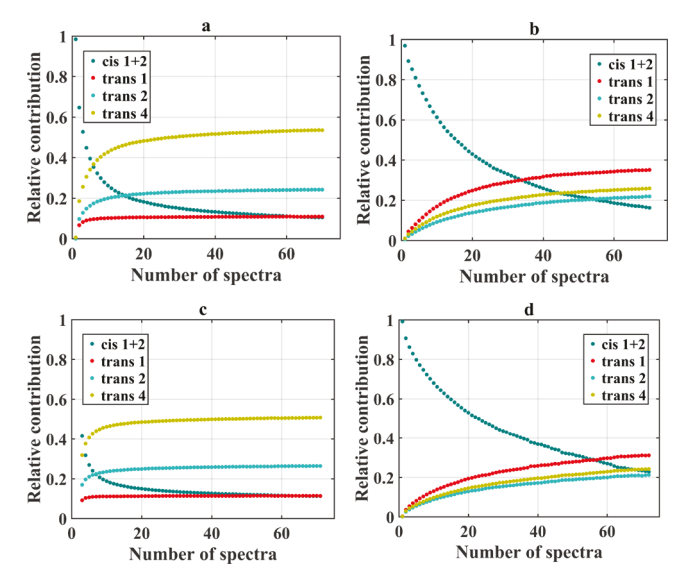


Figure 18. As in Figure 17. Product evolutions from spectra obtained in the course of the c-**2** \rightarrow t-**2** photoreactions for 300 (a, b) and 330 (c, d) nm excitation in FC (a, c) and SC (b, d) IP at 77 K. The % blue-shifted c-**2** conformer spectra in the initial spectra are 78, 49, 65, and 26 in (a), (b), (c), and (d), respectively.

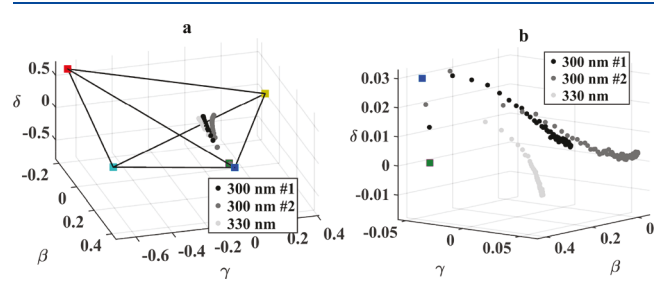


Figure 19. (a) Combination coefficient trajectories for two 300 nm and one 330 nm c-2 \rightarrow t-2 photoreactions in FC IP at 77 K. (b) As in (a) but zoomed.

Fluorescence Lifetimes of t-2 Conformers from c-2 in IP Glass at 77 K. The lifetimes obtained starting from c-2 in the IP glass are somewhat harder to interpret. Since multiple excitations are employed in order to reach 10 000 photon counts, we expect most of the fluorescence to originate from t-2 photoproduct conformers. At both excitation wavelengths the same three t-2 lifetimes are observed that were observed from the pure *t*-2 samples. In Table S3 with $\lambda_{\rm exc}$ = 370 nm, we find τ_1 = 1.01 \pm 0.09 ns, τ_2 = 1.66 \pm 0.10 ns, and τ_3 = 2.12 \pm 0.11 ns, and in Table S4 with $\lambda_{\rm exc}$ = 295 nm we find τ_1 = 1.09 \pm 0.04 ns, τ_2 = 1.62 \pm 0.16 ns, and τ_3 = 1.98 \pm 0.07 ns. In all cases, the latter two that correspond to the yellow and magenta spectra and were assigned to the s-trans, s-trans t-2 conformers dominate the decay curves. The difference in the composition of the fluorescence spectra from FC and SC IP glasses in Figure 17 is not observed in the decay curves. This reemphasizes the inability to reproduce IP glass environments using our experimental procedures. However, the lifetime measurements do confirm our conclusion that the $c-2 \rightarrow t-2$ photoreaction is slower in SC than in FC IP. Triexponential decay fits to the decays in SC IP revealed substantial contributions of lifetimes in the 0.03-0.30 ns range that probably were due to fluorescence from unreacted c-2 (Tables S3 and S4).

CONCLUSIONS

We confirmed the Froehlich and Morrison observation ¹⁵ of Stern–Volmer quenching of phosphorescence by 1,3-pentadiene in IP glass at 77 K. By monitoring the quencher concentration dependence of triplet lifetimes instead of phosphorescence intensity, we eliminated the possibility that static interactions play a role in this quenching. A rate constant of $2 \times 10^2 \, \mathrm{M}^{-1} \, \mathrm{s}^{-1}$ for translational quenching in this soft glass is consistent with the earlier observations and ours. We also observed phosphorescence quenching by O_2 in both IP and EPA confirming earlier preliminary results by Albrecht and coworkers in IP. ³⁶ The fact that O_2 quenching is roughly 5-fold faster than 1,3-pentadiene quenching is consistent with faster diffusion by the smaller solute.

We used c-2 and t-2 to show that the IP glass at 77 K traps unstable conformer photoproduct distributions as well as the much more rigid MCH glass. 17 Especially informative are comparisons of c-2 \rightarrow t-2 photoisomerization in FC and SC IP glasses. Very different distributions of c- 2_A and c- 2_B conformers are trapped depending on the cooling rate, and their photoisomerization leads to very different t-2 conformer mixtures. Theory predicts that $c-2_A$ should absorb to the red of c-2_B. Unfortunately, nearly identical resolved c-2 conformer fluorescence spectra do not allow definitive structure assignments, leaving the question of OBT vs HT photoisomerization mechanism unresolved. The conclusion that IP glass at 77 K permits translational diffusion but does not allow the torsional motions that would lead to conformer equilibration is not surprising when one considers that the conformers occupy shallow energy minima on the S₀ potential energy surface. While the translational diffusion of solutes is subject to the medium's activation energy for viscous flow, conformer equilibrations are subject to intrinsic activation energy barriers that are enhanced by the activation energy for viscous flow.⁴⁶

The demonstration that the IP glass at 77 K traps thermodynamically unstable conformer mixtures invalidates Liu's criticism¹³ of our interpretation of the photoisomerization of the cis isomers of 1,4-di-*o*-tolyl-1,3-butadiene. The conclusion that in IP glass at 77 K those photoisomerizations occur by the bicycle-pedal and OBT mechanisms and not by the HT mechanism stands.

ASSOCIATED CONTENT

S Supporting Information

The Supporting Information is available free of charge on the ACS Publications website at DOI: 10.1021/acs.jpca.9b07964.

TPE phosphorescence decay curves in MCH, EPA, and IP as a function of [t-P] at 77 K; quadratic fit of contraction of IP/3MP mixtures as a function of 3MP mole fraction on cooling from RT to 77 K; normalized fluorescence spectra of t-2 in fast and slower cooled IP at 77 K for $\lambda_{\rm exc}$ in the 300–370 nm range; first c-2 spectra in fast cooled IP at 77 K scanned from low to high and from high to low emission wavelength; fluorescence decay curves from t-2 and c-2 samples with $\lambda_{\rm exc} = 296$ and 370 nm, for FC and SC IP at 77 K; eigenvectors of the matrix composed of the spectra in Figure 4; combination coefficients of spectra in Figure 4 plotted in three vector spaces; four exponential fits to kinetic vectors V_1 - V_4 ; estimation of O_2 concentration in air saturated IP; results of theoretical calculations concerning interconversion of the s-trans, s-trans t-2 conformer pair; explanation of correction of fluorescence spectra for the buildup of photoproduct in the course of their acquisition; method to obtain spectral mixtures corresponding to the source of the consecutive exponential phases of the c-2 \rightarrow t-2 photoconversion; fluorescence lifetimes for t-2 in FC and SC IP and for t-2 photoproduct from c-2 in FC and SC IP (PDF)

AUTHOR INFORMATION

Corresponding Authors

*E-mail: zimanyi.laszlo@brc.mta.hu.

*E-mail: jsaltiel@fsu.edu.

ORCID

László Zimányi: 0000-0002-5101-2023 Jack Saltiel: 0000-0002-8680-2551

Author Contributions

László Zimányi performed the mathematical treatment of the spectra and contributed in the preparation of the manuscript. Sumesh B. Krishnan and Emily Williford contributed the experimental measurements concerning conformational trapping in IP. Shipra Gupta, Jonathan Sepulveda, and Hadleigh Schwartz contributed the experimental measurements concerning translational diffusion in IP. Frank B. Mallory and Clelia W. Mallory synthesized the *t-2* used in this work. Olga Dmitrenko performed the theoretical calculations. Jack Saltiel directed the research and prepared the manuscript for publication.

Notes

The authors declare no competing financial interest.

ACKNOWLEDGMENTS

Research at Florida State University was supported by the National Science Foundation, most recently by Grant No. CHE-1361962, and by Florida State University. E.W. was supported in part by National Science Foundation Research Experiences for Undergraduates Grant No. CHE-1659661. Research in the BRC, Szeged, was supported by the Hungarian Ministry for National Economy (Economic Development and Innovation Operational Program, GINOP-2.3.2-15-2016-00001).

DEDICATION

This paper is dedicated to the memory of Prof. Ugo Mazzucato and his seminal contributions to photochemistry.

REFERENCES

- (1) Saltiel, J.; Sun, Y.-P. Cis-Trans Isomerization of C,C Double Bonds. In *Photochromism, Molecules and Systems*; Dürr, H., Bouas-Laurent, H., Eds.; Elsevier: Amsterdam, 1990; pp 64–164.
- (2) Waldeck, D. H. Photoisomerization Dynamics of Stilbenes. Chem. Rev. 1991, 91, 415–436.
- (3) Liu, R. S. H.; Asato, A. E. Photochemistry of Polyenes. 22. The Primary Process of Vision and the Structure of Bathorhodopsin A Mechanism for Photoisomerization of Polyenes. *Proc. Natl. Acad. Sci. U. S. A.* 1985, 82, 259–263.
- (4) Liu, R. S. H.; Mead, D.; Asato, A. E. Application of the H.T.-n Mechanism of Photoisomerization to the Photocycles of Bacteriorhodopsin: A Model Study. *J. Am. Chem. Soc.* **1985**, *107*, 6609–6614.
- (5) Müller, A. M.; Lochbrunner, S.; Schmid, W. E.; Fuß, W. Low-Temperature Photochemistry of Previtamin D. A Hula-Twist Isomerization of a Triene. *Angew. Chem., Int. Ed.* **1998**, *37*, 505–507.

- (6) Redwood, C.; Bayda, M.; Saltiel, J. Photoisomerization of Preand Provitamin D₃ in EPA at 77 K: One Bond-Twist Not Hula-Twist. *J. Phys. Chem. Lett.* **2013**, *4*, 716–721.
- (7) Bayda, M.; Redwood, C. E.; Gupta, S.; Dmitrenko, O.; Saltiel, J. Lumisterol to Tachysterol Photoisomerization in EPA Glass at 77 K. A Comparative Study. *J. Phys. Chem. A* **2017**, *121*, 2331–234.
- (8) Liu, R. S. H.; Hammond, G. S. The Case of Medium-Dependent Dual Mechanisms for Photoisomerization: One-Bond-Flip and Hula-Twist. *Proc. Natl. Acad. Sci. U. S. A.* **2000**, *97*, 11153–11158.
- (9) Liu, R. S. H. Photoisomerization by Hula-Twist: A Fundamental Supramolecular Photochemical Reaction. *Acc. Chem. Res.* **2001**, *34*, 555–562.
- (10) Liu, R. S. H.; Hammond, G. S. Hula-Twist: A Photochemical Reaction Mechanism Involving Simultaneous Configurational and Conformational Isomerization. In *Handbook of Organic Photochemistry and Photobiology*, 2nd ed.; Horspool, W. M., Lenci, F., Eds.; CRC Press: London, 2004; Chapter 26, pp 1–11.
- (11) Yang, L.; Liu, R. S. H.; Boarman, K. J.; Wendt, N. L.; Liu, J. New Aspects of Diphenylbutadiene Photochemistry. Regiospecific Hula-Twist Photoisomerization. *J. Am. Chem. Soc.* **2005**, *127*, 2404–2405.
- (12) Saltiel, J.; Bremer, M. A.; Laohhasurayotin, S.; Krishna, T. S. R. Photoisomerization of cis,cis- and cis,trans-1,4-Di-o-tolyl-1,3-butadiene in Glassy Media at 77 K: One Bond Twist and Bicycle-Pedal. *Angew. Chem., Int. Ed.* **2008**, 47, 1237–1240.
- (13) Zhao, Y.-P.; Yang, L.-Y.; Simmons, C. J.; Liu, R. S. H. The Role of Organic Glasses in cis/trans Photoisomerization at Low Temperatures. *Chem. Asian J.* **2009**, *4*, 754–760.
- (14) Norman, I.; Porter, G. Trapped Atoms and Radicals in Rigid Solvents. *Proc. R. Soc. London Ser. A* 1955, 230, 399–414.
- (15) Froehlich, P.; Morrison, H. Phosphorescence Quenching by Diffusion in an Isopentane Glass. *J. Chem. Soc., Chem. Commun.* **1972**, 184–185.
- (16) Redwood, C.; Kumar, R. V. K.; Hutchinson, S.; Mallory, F. B.; Mallory, C. W.; Dmitrenko, O.; Saltiel, J. Four Component Fluorescence of *trans*-1,2-Di(1-methyl-2-naphthyl)ethene at 77 K in Glassy Media. Conformational Subtleties Revealed. *J. Phys. Chem. A* **2014**, *118*, 10575–10586.
- (17) Redwood, C.; Ratheesh Kumar, R. V.; Hutchinson, S.; Mallory, F. B.; Mallory, C. W.; Clark, R. J.; Dmitrenko, O.; Saltiel, J. Photoisomerization of *cis*-1,2-Di(1-methyl-2-naphthyl)ethene at 77 K in Glassy Media. *Photochem. Photobiol.* **2015**, *91*, 607–615.
- (18) Saltiel, J.; Kumar, R. V. K.; Redwood, C. E.; Mallory, F. B.; Mallory, C. W. Competing Adiabatic and Nonadiabatic Pathways in the Cis-Trans Photoisomerization of *cis*-1,2-Di(1-methyl-2-naphthyl)ethene. A Zwitterionic Twisted Intermediate. *Photochem. Photobiol. Sci.* **2014**, *13*, 172–181.
- (19) Herkstroeter, W. G.; Lamola, A. A.; Hammond, G. S. Mechanisms of Photochemical Reactions in Solution. XXVIII. Values of Triplet Excitation Energies of Selected Sensitizers. *J. Am. Chem. Soc.* **1964**, *86*, 4537–4540.
- (20) Casida, M. E.; Jamorski, C.; Casida, K. C.; Salahub, D. R. Molecular Excitation Energies to High-Lying Bound States from Time-Dependent Density-Functional Response Theory: Characterization and Correction of the Time-Dependent Local Density Approximation Ionization Threshold. J. Chem. Phys. 1998, 108, 4439–4449.
- (21) Stratmann, R. E.; Scuseria, G. E.; Frisch, M. J. An Efficient Implementation of Time-Dependent Density-Functional Theory for the Calculation of Excitation Energies of Large Molecules. *J. Chem. Phys.* 1998, 109, 8218–8224.
- (22) Boyle, N. M.; Vos, J. G. *GaussSum*, version 1.0.5; Dublin City University: Dublin, Ireland, 2005. Available at http://gausssum.sourceforge.net.
- (23) Bauernschmitt, R.; Ahlrichs, R. Treatment of Electronic Excitations within the Adiabatic Approximation of Time Dependent Density Functional Theory. *Chem. Phys. Lett.* **1996**, 256, 454–464.
- (24) Furche, F.; Ahlrichs, R. Adiabatic Time-Dependent Density Functional Methods for Excited State Properties. *J. Chem. Phys.* **2002**, 117, 7433–7447.

- (25) Casida, M. E.; Jamorski, C.; Casida, K. C.; Salahub, D. R. Molecular Excitation Energies to High-Lying Bound States from Time-Dependent Density-Functional Response Theory: Characterization and Correction of the Time-Dependent Local Density Approximation Ionization Threshold. *J. Chem. Phys.* **1998**, *108*, 4439–4449.
- (26) Caricato, M.; Trucks, G. W.; Frisch, M. J.; Wiberg, K. B. Oscillator Strength: How Does TDDFT Compare to EOM-CCSD? *J. Chem. Theory Comput.* **2011**, *7*, 456–466.
- (27) Klyne, W.; Prelog, V. Description of Steric Relationships across Single Bonds. *Experientia* **1960**, *16*, 521–523.
- (28) Testa, B.; Vistoli, G.; Pedretti, A. Organic Stereochemistry Part 4. Isomerisms about Single Bonds and in Cyclic Systems. *Helv. Chim. Acta* **2013**, *96*, 564–623.
- (29) McClure, D. S. Triplet-Singlet Transitions in Organic Molecules. Lifetime Measurements of the Triplet State. *J. Chem. Phys.* **1949**, *17*, 905–913.
- (30) Azumi, T.; McGlynn, S. P. Delayed Fluorescence of Solid Solutions of Polyacenes. Kinetic Considerations. *J. Chem. Phys.* **1963**, 39, 1186–1194.
- (31) Morgan, D. M.; Warschawsky, D.; Atkinson, T. The Relationship between Carcinogenic Activities of Polycyclic Aromatic Hydrocarbons and Their Singlet, Triplet, and Singlet-Triplet Splitting Energies and Phosphorescence Lifetimes. *Photochem. Photobiol.* **1977**, 25, 31–38.
- (32) Offen, H. W.; Hein, D. E. Environmental Effects on Phosphorescence. Matrix Site Effects for Triphenylene. *J. Chem. Phys.* **1969**, *50*, 5274–5279.
- (33) IUPAC Analytical Chemistry Division, Commission on Solubility Data, Oxygen and Ozone. In *Solubility Data Series*; Battino, R., Ed.; Pergamon: Oxford, U.K., 1981; Vol. 7, p 286.
- (34) Handbook of Chemistry, 9th ed.; Lange, N. A., Ed.; Handbook Publishers, Inc.: Sandusky, OH, 1956; p 1435.
- (35) Ling, A. C.; Willard, J. E. Viscosities of Some Organic Glasses Used as Trapping Matrices. *J. Phys. Chem.* **1968**, 72, 1918–1923.
- (36) Lombardi, J. R.; Raymonda, J. W.; Albrecht, A. C. Rotational Relaxation in Rigid Media by Polarized Photoselection. *J. Chem. Phys.* **1964**, *40*, 1148–1156.
- (37) Rosengren, Kj. A Study on Contraction, Relative Viscosity and Melting Curves of Some Glass-forming Hydrocarbon Mixtures. *Acta Chem. Scand.* **1962**, *16*, 1421–1425.
- (38) Saltiel, J.; Atwater, B. W. Spin-Statistical Factors in Diffusion-Controlled Reactions. *Adv. Photochem.* **2007**, *14*, 1–90.
- (39) Sun, Y.-P.; Saltiel, J. Application of the Kramers Equation to Stilbene Photoisomerization in n-Alkanes Using Translational Diffusion Coefficients to Define Microviscosity. *J. Phys. Chem.* **1989**, 93, 8310–8316.
- (40) Greenspan, H.; Fischer, E. Viscosities of Glass-Forming Solvent Mixtures at Low Temperatures. *J. Phys. Chem.* **1965**, *69*, 2466–2469.
- (41) Havinga, E.; Schlatmann, J. L. M. A. Remarks on the Specificities of the Photochemical and Thermal Transformations in the Vitamin D Field. *Tetrahedron* **1961**, *16*, 146–152.
- (42) Havinga, E. Über Einige Photochemische Reactionen. *Chimia* **1962**, *16*, 145–172.
- (43) Jacobs, H. J. C.; Havinga, E. Photochemistry of Vitamin D and its Isomers and of Simple Trienes. *Adv. Photochem.* **2007**, *11*, 305–373.
- (44) Lawton, W. H.; Sylvestre, E. A. Self Modeling Curve Resolution. *Technometrics* 1971, 13, 617–633.
- (45) Lawton, W. H.; Sylvestre, E. A.; Maggio, M. S. Curve Resolution Using a Postulated Chemical Reaction. *Technometrics* 1974, 16, 353–368.
- (46) Saltiel, J.; Sun, Y.-P. The Intrinsic Potential Energy Barrier for Twisting in the trans-Stilbene S1 State in Hydrocarbon Solvents. *J. Phys. Chem.* **1989**, 93, 6246–6250.